

The globular cluster VVV CL002 falling down to the hazardous Galactic centre

Dante Minniti^{1,2,3}, Noriyuki Matsunaga^{4,5}, José G. Fernández-Trincado⁶, Shogo Otsubo⁵, Yuki Sarugaku⁵, Tomomi Takeuchi⁵, Haruki Katoh⁵, Satoshi Hamano⁷, Yuji Ikeda^{5,8}, Hideyo Kawakita^{5,9}, Philip W. Lucas¹⁰, Leigh C. Smith¹¹, Iliaria Petralia¹, Elisa Rita Garro¹, Roberto K. Saito³, Javier Alonso-García¹², Matías Gómez¹, and María Gabriela Navarro¹³

- ¹ Instituto de Astrofísica, Depto. de Ciencias Físicas, Facultad de Ciencias Exactas, Universidad Andres Bello, Fernandez Concha 700, Santiago, RM, Chile
e-mail: dante.minniti@unab.cl
- ² Specola Vaticana, Vatican Observatory, Castelgandolfo, V00120, Stato Citta Vaticano, Italy
- ³ Departamento de Física, Universidade Federal de Santa Catarina, Florianopolis, Trindade 88040-900, SC, Brazil
- ⁴ Department of Astronomy, School of Science, The University of Tokyo, 7-3-1 Hongo, Bunkyo-ku, Tokyo 113-0033, Japan
e-mail: matsunaga@astron.s.u-tokyo.ac.jp
- ⁵ Laboratory of Infrared High-resolution Spectroscopy (LiH), Koyama Astronomical Observatory, Kyoto Sangyo University, Motoyama, Kamigamo, Kita-ku, Kyoto 603-8555, Japan
- ⁶ Instituto de Astronomía, Universidad Católica del Norte, Av. Angamos 0610, Antofagasta, Chile
- ⁷ National Astronomical Observatory of Japan, 2-21-1 Osawa, Mitaka, Tokyo 181-8588, Japan
- ⁸ Photocoding, 460-102 Iwakura-Nakamachi, Sakyo-ku, Kyoto 606-0025, Japan
- ⁹ Department of Astrophysics and Atmospheric Sciences, Faculty of Science, Kyoto Sangyo University, Motoyama, Kamigamo, Kita-ku, Kyoto 603-8555, Japan
- ¹⁰ Centre for Astrophysics Research, University of Hertfordshire, College Lane, Hatfield, AL10 9A, United Kingdom
- ¹¹ Institute of Astronomy, University of Cambridge, Madingley Rd., Cambridge, CB3 0HA, United Kingdom
- ¹² Centro de Astronomia (CITEVA), Universidad de Antofagasta, Av. Angamos 601, Antofagasta, Chile
- ¹³ INAF, Osservatorio Astronomico di Roma, Via di Frascati 33, Monteporzio Catone, 00040, Italy

Received Month DD, Year; accepted Month DD, Year

ABSTRACT

Context. The Galactic centre is hazardous for stellar clusters because of the strong tidal force. Supposedly, many clusters were destroyed and contributed stars to the crowded stellar field of the bulge and the nuclear stellar cluster. However, it is hard to develop a realistic model to predict the long-term evolution of the complex inner Galaxy, and observing surviving clusters in the central region would provide crucial insights into destruction processes.

Aims. Among hitherto-known Galactic globular clusters, VVV CL002 is the closest to the centre, 0.4 kpc, but has a very high transverse velocity, 400 km s⁻¹. The nature of this cluster and its impact on Galactic astronomy need to be addressed with spectroscopic follow-up.

Methods. Here we report the first measurements of its radial velocity and chemical abundance based on near-infrared high-resolution spectroscopy.

Results. We found that this cluster has a counterrotating orbit constrained within 1.0 kpc of the centre, as close as 0.2 kpc at the perigalacticon, confirming that the cluster is not a passerby from the halo but a genuine survivor enduring the harsh conditions of the Galactic mill's tidal forces. In addition, its metallicity and α abundance ($[\alpha/\text{Fe}] \approx +0.4$ and $[\text{Fe}/\text{H}] = -0.54$) are similar to some globular clusters in the bulge. Recent studies suggest that stars with such α -enhanced stars were more common at 3–6 kpc from the centre around 10 Gyrs ago.

Conclusions. We infer that VVV CL002 was formed outside but is currently falling down to the centre, exhibiting a real-time event that must have occurred to many clusters a long time ago.

Key words. giant planet formation – κ -mechanism – stability of gas spheres

1. Introduction

Whereas more than 200 globular clusters have been found today in the Galaxy, there is plenty of evidence for clusters having been destroyed by various evolutionary and dynamical processes, including dynamical friction, shocking by disk and bulge, tidal disruption, and so on (Leon et al. 2000; Murali & Weinberg 1997; Gnedin & Ostriker 1997; Baumgardt & Makino 2003; Moreno et al. 2022). Many of these dynamical processes are stronger

in the deep potential well of the inner Galaxy. Numerical simulations have revealed that the supermassive black hole Sagittarius A* (Ghez et al. 2008; Genzel et al. 2010) is a very efficient machine of grinding clusters, where globular clusters could be rapidly demolished (Arca-Sedda & Capuzzo-Dolcetta 2017; Navarro et al. 2023). In order to address the process of globular cluster disruption, it is crucial to understand not only clusters that have been destroyed but also surviving globular clusters. Search for globular clusters in the inner Galaxy has been incomplete

because of large interstellar extinction and heavy source crowding, Still, recent near-infrared surveys have revealed dozens of candidate clusters in the inner bulge (Moni Bidin et al. 2011; Borissova et al. 2014). Then, confirmation of member stars and detailed characterization of the clusters' properties require infrared spectroscopic observations due to large interstellar extinction near the centre.

VVV CL002 is a relatively low-luminosity globular cluster ($M_K = -7.1$ mag, $M_V = -4.6$ mag (Minniti et al. 2021)), which was discovered at 1.1 deg from the Galactic centre through the VISTA Variables in the Via Lactea (VVV) survey (Moni Bidin et al. 2011). The distance measured with the red clump places this cluster closest to the centre, 0.4 kpc, among known globular clusters, and an additional surprise is the high transverse velocity, 400 km s^{-1} , inferred from the proper motion (Minniti et al. 2021). A part of RR Lyr variables with such high velocities found in the bulge turned out to be halo objects (Kunder et al. 2020). Is VVV CL002 an interloper from the halo passing near the Galactic centre? If it remains near the centre instead, we need to consider how it is surviving without being tidally disrupted. Spectroscopic observations are required to answer these questions.

2. Observation and data analysis

2.1. Target selection

Embedded in the crowded stellar field, selecting good targets for follow-up spectroscopic observations is a crucial step. In particular, the cluster membership determination is very tricky in such a crowded field (Fig. 1). The line-of-sight contamination of stars in various groups increase at low latitudes, and accurate 6D information (position, radial velocity and proper motion) is vital in judging membership. Based on the VVV's photometry and proper motions in the updated VIRAC2 database (Smith et al., in prep) we selected a few candidate members of red giant (Fig. 2) including the two stars that we actually observed. Therefore we initially selected the four brightest RGB stars with high probability of membership according to the photometric and astrometric data. The main criteria for the selection of this sample were: 1) Stars within 0.1 mag from the mean RGB ridge line in the near-IR color-magnitude diagram. 2) Stars with PMs within 0.1 mas/yr from the mean GC PM. 3) Stars that appeared unblended in the optical and near-IR images. 4) Stars brighter than $J = 14.2$ mag. Two out of these four main targets selected were successfully observed (Table 1). The remaining two targets could not be observed due to time and weather constraints during our observing run. These are Gaia ID 9327562004074, with $K_s=11.87$ mag, $J-K_s=2.22$ mag; and Gaia ID 9327562025638, with $K_s=11.90$ mag, $J-K_s=2.24$ mag, which would also be prime targets for future spectroscopic observations. The proper motions of candidate members of VVV CL002 show a large offset from the bulk of bulge field stars, which indicates the large transverse velocity of the clusters, $\sim 400 \text{ km s}^{-1}$ (Minniti et al. 2021). Although some contaminants remain, stars selected by the proper motion show the red giant branch and red clump expected for a globular cluster.

2.2. Observation

On June 10th, 2023, we used the WINERED spectrograph (Ikeda et al. 2022; Matsunaga et al. 2023) attached to the Magellan Clay telescope in Chile to obtain high-resolution spectra of two stars. WINERED is a near-IR high-resolution spectrograph cov-



Fig. 1. Near-infrared image of the field around VVV CL002 made with VVV images in the JHK_s -band filters, indicating the target red giant stars A (VIRAC2 ID=9327562027332) and B (VIRAC2 ID=9327562015390). The field covers $4' \times 3'$, oriented along Galactic coordinates, with latitude increasing upwards and longitude to the left. The globular cluster is located at the centre of this image, that also illustrates the overwhelming density of field stars.

ering $0.90\text{--}1.35 \mu\text{m}$ (z' , Y , and J bands), with a resolution of $R = \lambda/\Delta\lambda = 28,000$ with the WIDE mode (Ikeda et al. 2022). The raw spectral data were reduced with the WINERED Automatic Reduction Pipeline (WARP¹, version 3.8). We confirmed that the broadening width in the final spectra is as small as 12 km s^{-1} , which can be explained by the combination of the instrumental resolution (10.7 km s^{-1}) and a typical macroturbulence of about 5 km s^{-1} . These stars are the brightest among a few targets that were selected as candidate members. The two stars are the brightest, $J \approx 13.5$ mag, of the targets we selected, but they are rather faint targets for high-resolution spectroscopy in the infrared. Our spectra with 1200s exposures for each star are of moderate quality. While the signal-to-noise ratios are $S/N = 30\text{--}50$ in the J band, they are $15\text{--}20$ in the Y band (shorter wavelengths) because of severe interstellar extinction. Therefore, our analysis relied mainly on the J -band part of the spectra (Fig. 3). The spectra of the two stars show a striking resemblance to each other (Fig. 3), with the same absorption lines appearing at the same wavelengths and exhibiting very similar depths. This already indicates that the two target stars are red giants with very similar characteristics, belonging to a common stellar group, VVV CL002.

2.3. Measurements of radial velocities

We measured radial velocities using the cross correlation technique involving the model synthetic spectra and telluric absorption spectra (Matsunaga et al. 2015). For this analysis, we include some Y -band echelle orders together with J -band orders, in which telluric lines and stellar lines are well mixed. We obtained almost identical velocities for the two stars (Table 1), strongly supporting the membership to VVV CL002 combined with the proper motions (Fig. 2).

2.4. Measurements of chemical abundances

In spite of the limited S/N, we are able to measure the abundances of Fe, Mg, and Si. First, we estimated the effective

¹ <https://github.com/SatoshiHamano/WARP/>

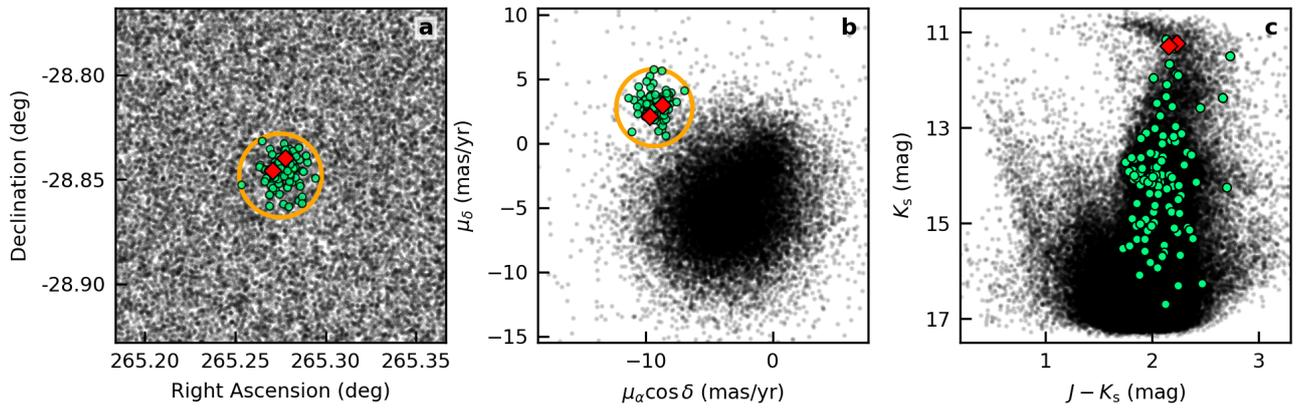


Fig. 2. Illustration of the target selection from VVV CL002: (a) the field surrounding the cluster, (b) the proper motion diagram, and (c) the near-IR color-magnitude diagram. The field stars are plotted with the black points, while stars located inside the selection circles (orange) on both the panels (a) and (b) are indicated by green circles. A part of these stars in green were selected as spectroscopic targets based also on panel (c), and we observed the two red giants indicated by red diamonds.

Table 1. Observed target stars and mean globular cluster parameters

Parameter	Star A	Star B	Mean
ID (VIRAC2)	9327562027332	9327562015390	
RA (J2000)	17:41:06.65	17:41:04.94	
Dec (J2000)	-28:50:23.1	-28:50:44.4	
K_s (mag)	11.25	11.21	
$J-K_s$ (mag)	2.20	2.25	
V_{helio} (km s $^{-1}$)	-27.3 ± 0.2	-27.3 ± 0.2	-27.3 ± 0.1
V_{LSR} (km s $^{-1}$)	-17.0 ± 0.2	-17.1 ± 0.2	-17.1 ± 0.1
[Fe/H]	-0.68 ± 0.37	-0.39 ± 0.41	-0.54 ± 0.27
[Mg/H]	-0.26 ± 0.19	-0.14 ± 0.12	-0.19 ± 0.10
[Si/H]	-0.12 ± 0.29	-0.02 ± 0.25	-0.07 ± 0.19

temperature employing the line-depth ratios (Taniguchi et al. 2018). We could measure the ratios of 6–7 line pairs taken from Taniguchi et al. (2018) as illustrated in Fig. 4. Adopting an error of 200 K, we use the approximate value of the temperatures, $T_{\text{eff}} = 4100$ K, for both stars in the following analysis. It is impossible to determine other stellar parameters due to the limited quality of the current spectra. Considering the similarity to Arcturus, we used the following parameters: $\log g = 1.5$, and the microturbulent velocity $\xi = 1.5$ km s $^{-1}$ (Fukue et al. 2021).

Then, we determined the chemical abundances by fitting model spectra to individual absorption lines that were isolated from telluric lines and other strong stellar lines. The measurements were successfully done for about 10 Fe I lines, 7 Si lines, and 4 Mg lines, leading to the abundances listed in Table 1. The errors in the [X/H] values of individual stars are given by the combination of the standard deviations of the line-by-line abundances and the systematic errors caused by uncertainties in stellar parameters such as T_{eff} . The line-by-line random errors dominate the total errors in all cases, i.e., the three elements in the two stars. Among the systematic errors, the errors from the $\log g$ uncertainty tends to be the largest error source, 0.6–0.9 dex in [X/H], but the T_{eff} uncertainty has the highest impact in [Si/H], ~ 0.1 dex. The trends of the systematic errors are similar to what was found for Arcturus (Fig. 7 in Fukue et al. 2021), but the errors in each stellar parameter, especially $\log g$, are significantly larger for our targets. Finally, we took weighted means and their errors of the [X/H] values of the two stars to discuss the chemical abundances of the cluster (Table 1). In fact, we obtained almost identical velocities and common chemical abun-

dances within the errors for the two stars (Table 1). Such close agreements are unexpected for field stars in the bulge characterized by a large velocity dispersion and a wide metallicity distribution (Recio-Blanco 2018; Zasowski et al. 2019; Schultheis et al. 2020; Geisler et al. 2021; Queiroz et al. 2021). In addition, the spectra of these two stars are similar to the high S/N spectrum of the prototype red giant Arcturus ([Mg/H] = -0.2 , [Si/H] = -0.2 , [Fe/H] = -0.5 (Fukue et al. 2021)), supporting the metallicities and the α enhancement of our two stars. There are absorption lines of some other elements seen in the obtained spectra, as indicated in Fig. 1. It would be valuable to measure the abundances of such elements, but we limited ourselves to the three elements (Fe, Si, Mg) for which simple analysis with the limited-S/N spectra was sufficient. For example, the number of useful Ca lines is more limited than Mg because of blends by telluric lines and stellar lines and also because only a few lines have moderate depths appropriate with the limited S/N values. Ti tends to be affected by NLTE. Measuring C and/or N abundances with CN would require CO and OH lines together, but none of these lines are available in the WINERED range.

3. Cluster orbit

We computed the orbit using the 3D barred Galaxy steady-state potential model of the GravPot16 code (Fernández-Trincado et al. 2022). We ran the orbital simulation considering different bar pattern speeds, $\Omega_{\text{bar}} = 31, 41, \text{ and } 51$ km s $^{-1}$ kpc $^{-1}$ (Sanders et al. 2019). For VVV CL002, we obtained 10,000 orbits adopting a simple Monte Carlo re-sampling, where the uncertainties in the input coordinates (α, δ), proper motions, radial velocities, and distance errors were randomly propagated as 1σ variations in the Gaussian Monte Carlo re-sampling. Fig. 5 shows the computed orbits using $\Omega_{\text{bar}} = 41$ km s $^{-1}$ kpc $^{-1}$, displayed as probability densities of orbits projected on the equatorial Galactic plane (left panel) and height above the plane z vs Galactocentric radius in kpc (right panel). The lighter colours indicate more probable regions of space, that are travelled more frequently by the simulated orbits. According to the result of this calculation, VVV CL002 has a retrograde orbital configuration of relatively high eccentricity ($e = 0.69 \pm 0.22$), with perigalactocentric and apogalactocentric distances well inside the Galactic bulge at $R_{\text{peri}} = 0.19 \pm 0.21$ kpc and $R_{\text{apo}} = 1.04 \pm 0.29$ kpc, respectively, and with moderate vertical excursions from the Galactic plane ($|Z_{\text{max}}| = 0.35 \pm 0.09$ kpc). It is important to note that any adopted

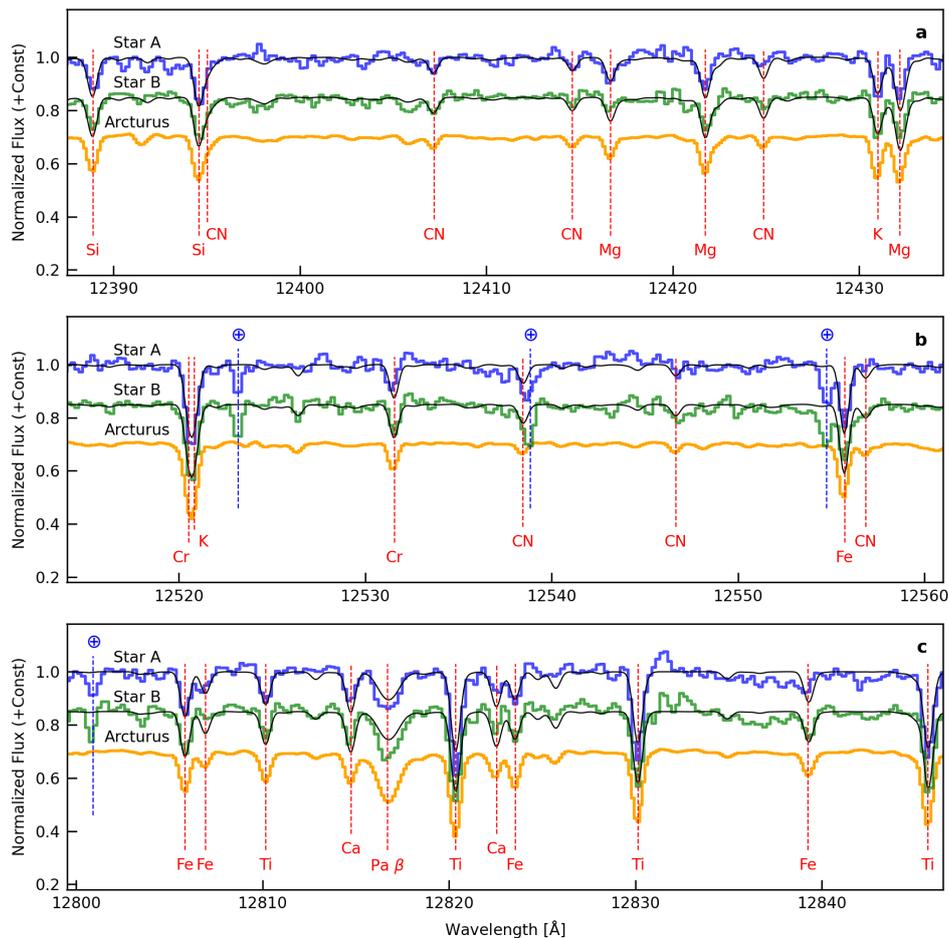


Fig. 3. Spectra for the two red giant members of the globular cluster VVV CL002: star A in blue and star B in green. Three representative parts containing absorption lines used for abundance measurements (Mg, Si, and Fe) and other lines are presented together with model spectra synthesized with $T_{\text{eff}} = 4100$ K, $\log g = 1.5$ and $[\text{Fe}/\text{H}] = -0.54$ (black). The spectrum of Arcturus (orange) is also shown for comparison, shifted to the appropriate velocity to match with the spectra of target stars. Arcturus ($T_{\text{eff}} = 4280$ K, $[\text{Mg}/\text{H}] = -0.2$, $[\text{Si}/\text{H}] = -0.2$, $[\text{Fe}/\text{H}] = -0.5$) is a prototype red giant observed with the same setup (Fukue et al. 2021). Note that all the spectra look very similar to each other. Absorption lines with the \oplus mark show telluric lines, which are only seen in the two target stars but not in Arcturus for which the telluric correction was done.

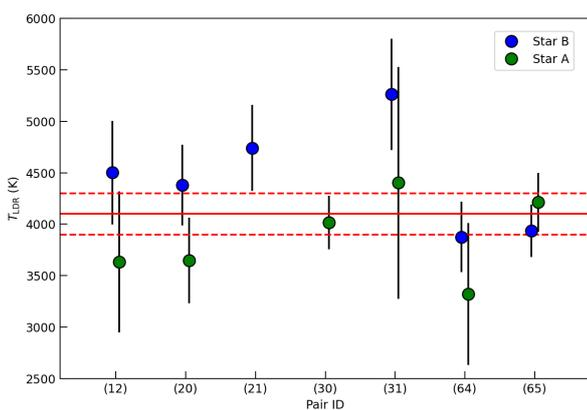


Fig. 4. LDR-based temperatures estimated with line pairs taken from Taniguchi et al. (2018). The solid and dashed lines indicate the temperature and its error used for measuring chemical abundances of the two stars.

heliocentric distance, our simulations confirm that kinematically VVV CL002 now belongs to the bulge, instead of being a halo globular cluster in a very eccentric orbit that is merely passing by the inner bulge.

4. Discussion

The radial velocity we obtained allows to give a strong constraint to the full 3D motion of the cluster. We calculated 10,000 orbits of VVV CL002, adopting a Monte Carlo re-sampling with the uncertainties in input parameters such as distance, radial velocity and proper motion taken into account. We found that VVV CL002 has a retrograde orbital configuration of relatively high eccentricity ($e = 0.69 \pm 0.22$), with perigalactocentric and apogalactocentric distances well inside the bulge, $R_{\text{peri}} = 0.19$ kpc and $R_{\text{apo}} = 1.04$ kpc (Fig. 5). The retrograde motion is not unique, as there exist a few other retrograde globular clusters enduring the harsh density of the Galactic bulge (Romero-Colmenares et al. 2021; Pérez-Villegas et al. 2020; Garro et al. 2023). However, the orbit of VVV CL002 is tighter than the orbits of all other known globular clusters (Pérez-Villegas et al. 2020). No globular cluster is expected to survive over its life-

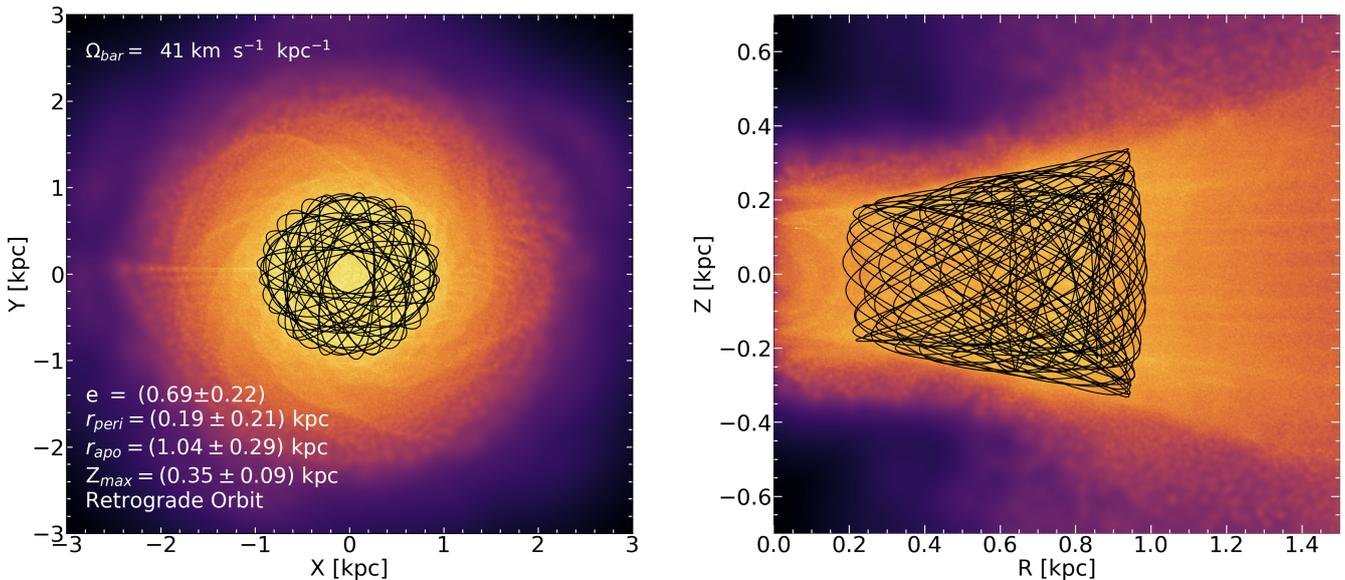


Fig. 5. Orbit computed for VVV CL002 (black line), overlaid on the probability densities of orbits projected on the Galactic plane (left) and height above the plane z versus Galactocentric radius (right). Lighter colours indicate more probable regions of space, that are more frequently sampled by the simulated orbits.

time (>10 Gyr) in such proximity to the Galactic centre (Gnedin et al. 2014).

In order to unveil the mysterious history of this cluster, its chemical abundance plays an essential role. The abundances of the two stars agree within the errors, giving an estimate of the cluster’s metallicity, $[\text{Fe}/\text{H}] = -0.54 \pm 0.27$, consistent with a previous photometric determination ($[\text{Fe}/\text{H}] = -0.4$, (Moni Bidin et al. 2011)), and $[\alpha/\text{Fe}] \approx +0.4$ (Table 1). The high α enhancement is connected to rapid chemical evolution dominated by core-collapse supernovae rather than type Ia supernovae (Sharma et al. 2021). This confirms that VVV CL002 is an old globular cluster formed together with other clusters and field stars present today in the Galactic bulge (Fig. 6), rather than a younger open cluster or the remains from an (already-disrupted) dwarf galaxy (Hughes et al. 2020). Furthermore, using a state-of-the-art technique for estimating stellar birth radii (R_{birth}) within the Galaxy (Minchev et al. 2018), recent studies demonstrated that stars with relatively low metallicity (among bulge stars) and high α enhancement were formed more in the outer part, 3–6 kpc in R_{birth} (Lu et al. 2022; Ratcliffe et al. 2023). This brings us to a scenario where VVV CL002 was formed at a relatively large R_{birth} and started to fall towards the centre recently. It is probably doomed to continue spiralling into the inner parsecs and be destroyed in the not-so-distant future. This cluster sheds light on the intriguing survival and migration mechanisms of globular clusters, whereas many less-characterized globular clusters and candidates are within a couple of kilo-parsecs from the centre. Demand is high for near-infrared high-resolution spectroscopy of such clusters, which has been handicapped due to severe interstellar extinction.

Acknowledgements. This paper is based on the WINERED data gathered with the 6.5 meter Magellan Telescope located at Las Campanas Observatory, Chile. This research is supported by JSPS Bilateral Program Number JPJSBP120239909. The observing run in 2023 June was partly supported by KAKENHI (grant No 18H01248). We also acknowledge Scarlet S. Elgueta and Rogelio R. Albarracín for supporting the observations. WINERED was developed by the University of Tokyo and the Laboratory of Infrared High-resolution Spectroscopy, Kyoto Sangyo University, under the financial support of KAKENHI (Nos. 16684001, 20340042, and 21840052) and the MEXT Supported Program for the Strategic Research Foundation at Private Universities (Nos.

S0801061 and S1411028). We gratefully acknowledge the use of data from the ESO Public Survey program IDs 179.B-2002 and 198.B-2004 taken with the VISTA telescope and data products from the Cambridge Astronomical Survey Unit. D.M. acknowledges support by the ANID BASAL projects ACE210002 and FB210003, by Fondecyt Project No. 1220724, and by CNPq/Brazil through project 350104/2022-0. J.G.F.-T. acknowledges support provided by Agencia Nacional de Investigación y Desarrollo de Chile (ANID) under the Proyecto Fondecyt Iniciación 2022 Agreement No. 11220340, and from the Joint Committee ESO-Government of Chile 2021 under the Agreement No. ORP 023/2021, and from Becas Santander Movilidad Internacional Profesores 2022, Banco Santander Chile. R.K.S. acknowledges support from CNPq/Brazil through projects 308298/2022-5 and 350104/2022-0. E.R.G. acknowledges support from ANID PhD scholarship No. 21210330.

References

- Abdurro’uf, Accetta, K., Aerts, C., et al. 2022, *ApJS*, 259, 35
 Arca-Sedda, M. & Capuzzo-Dolcetta, R. 2017, *MNRAS*, 471, 478
 Barbuy, B., Cantelli, E., Muniz, L., et al. 2021, *A&A*, 654, A29
 Barbuy, B., Chiappini, C., & Gerhard, O. 2018, *ARA&A*, 56, 223
 Baumgardt, H. & Makino, J. 2003, *MNRAS*, 340, 227
 Borissova, J., Chené, A. N., Ramírez Alegría, S., et al. 2014, *A&A*, 569, A24
 Carretta, E., Bragaglia, A., Gratton, R., & Lucatello, S. 2009, *A&A*, 505, 139
 Dias, B., Barbuy, B., Saviane, I., et al. 2016, *A&A*, 590, A9
 Fernández-Trincado, J. G., Beers, T. C., Barbuy, B., et al. 2022, *A&A*, 663, A126
 Fukue, K., Matsunaga, N., Kondo, S., et al. 2021, *ApJ*, 913, 62
 Garro, E. R., Fernández-Trincado, J. G., Minniti, D., et al. 2023, *A&A*, 669, A136
 Geisler, D., Villanova, S., O’Connell, J. E., et al. 2021, *A&A*, 652, A157
 Genzel, R., Eisenhauer, F., & Gillessen, S. 2010, *Reviews of Modern Physics*, 82, 3121
 Ghez, A. M., Salim, S., Weinberg, N. N., et al. 2008, *ApJ*, 689, 1044
 Gnedin, O. Y. & Ostriker, J. P. 1997, *ApJ*, 474, 223
 Gnedin, O. Y., Ostriker, J. P., & Tremaine, S. 2014, *ApJ*, 785, 71
 Hughes, M. E., Pfeffer, J. L., Martig, M., et al. 2020, *MNRAS*, 491, 4012
 Ikeda, Y., Kondo, S., Otsubo, S., et al. 2022, *PASP*, 134, 015004
 Kunder, A., Pérez-Villegas, A., Rich, R. M., et al. 2020, *AJ*, 159, 270
 Leon, S., Meylan, G., & Combes, F. 2000, *A&A*, 359, 907
 Lu, Y., Minchev, I., Buck, T., et al. 2022, arXiv e-prints, arXiv:2212.04515
 Matsunaga, N., Fukue, K., Yamamoto, R., et al. 2015, *ApJ*, 799, 46
 Matsunaga, N., Taniguchi, D., Elgueta, S. S., et al. 2023, arXiv e-prints, arXiv:2308.02853
 Mészáros, S., Masseron, T., García-Hernández, D. A., et al. 2020, *MNRAS*, 492, 1641
 Minchev, I., Anders, F., Recio-Blanco, A., et al. 2018, *MNRAS*, 481, 1645
 Minniti, D., Fernández-Trincado, J. G., Smith, L. C., et al. 2021, *A&A*, 648, A86

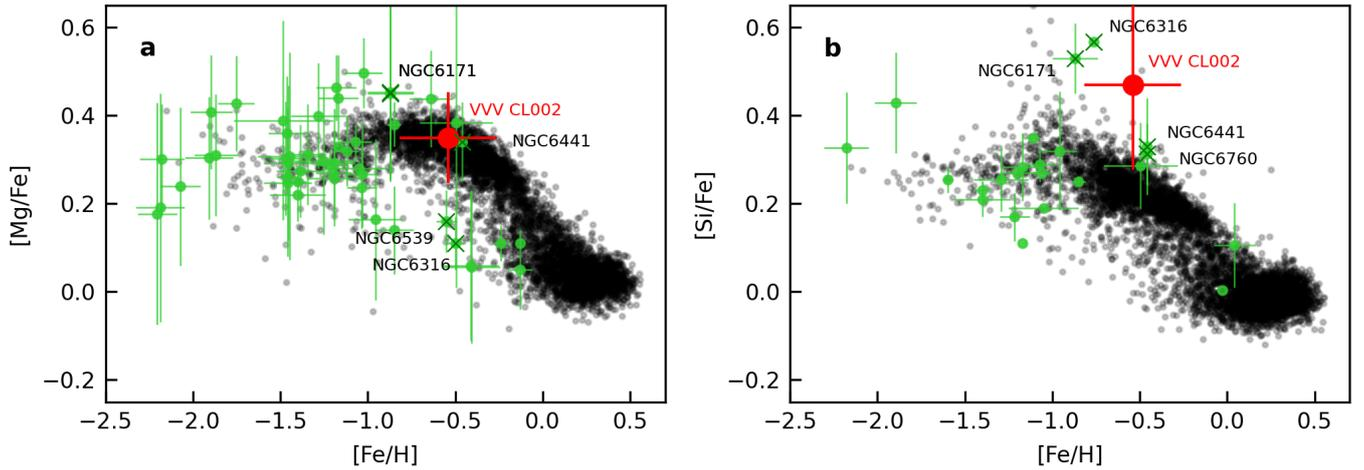


Fig. 6. $[\text{Mg}/\text{Fe}]$ versus $[\text{Fe}/\text{H}]$ (left) and $[\text{Si}/\text{Fe}]$ versus $[\text{Fe}/\text{H}]$ (right) for the globular cluster VVV CL002 (red circle) compared with the abundances of other known globular clusters indicated by green circles (Mészáros et al. 2020; Carretta et al. 2009; Dias et al. 2016; Recio-Blanco 2018; Barbuy et al. 2018, 2021; Geisler et al. 2021; Schiavon et al. 2023) and bulge field stars indicated by small dots (Abdurro’uf et al. 2022; Queiroz et al. 2023) The globular cluster mean abundances with their respective errors are all from mid/high resolution optical and IR spectroscopy from the literature as compiled by Garro et al. (2023, submitted). Also a few representative globular clusters that bracket the VVV-CL002 abundances are marked with crosses and labelled for comparison.

Moni Bidin, C., Mauro, F., Geisler, D., et al. 2011, *A&A*, 535, A33
 Moreno, E., Fernández-Trincado, J. G., Pérez-Villegas, A., Chaves-Velasquez, L., & Schuster, W. J. 2022, *MNRAS*, 510, 5945
 Murali, C. & Weinberg, M. D. 1997, *MNRAS*, 288, 749
 Navarro, M. G., Capuzzo-Dolcetta, R., Arca-Sedda, M., & Minniti, D. 2023, *A&A*, 674, A148
 Pérez-Villegas, A., Barbuy, B., Kerber, L. O., et al. 2020, *MNRAS*, 491, 3251
 Queiroz, A. B. A., Anders, F., Chiappini, C., et al. 2023, *A&A*, 673, A155
 Queiroz, A. B. A., Chiappini, C., Perez-Villegas, A., et al. 2021, *A&A*, 656, A156
 Ratcliffe, B., Minchev, I., Anders, F., et al. 2023, *MNRAS*[arXiv:2305.13378]
 Recio-Blanco, A. 2018, *A&A*, 620, A194
 Romero-Colmenares, M., Fernández-Trincado, J. G., Geisler, D., et al. 2021, *A&A*, 652, A158
 Sanders, J. L., Smith, L., & Evans, N. W. 2019, *MNRAS*, 488, 4552
 Schiavon, R. P., Phillips, S. G., Myers, N., et al. 2023, *MNRAS*[arXiv:2310.07764]
 Schultheis, M., Rojas-Arriagada, A., Cunha, K., et al. 2020, *A&A*, 642, A81
 Sharma, S., Hayden, M. R., & Bland-Hawthorn, J. 2021, *MNRAS*, 507, 5882
 Taniguchi, D., Matsunaga, N., Kobayashi, N., et al. 2018, *MNRAS*, 473, 4993
 Zasowski, G., Schultheis, M., Hasselquist, S., et al. 2019, *ApJ*, 870, 138